RESEARCH ARTICLE | AUGUST 05 2022

Ohmic co-doped GaN/InGaN tunneling diode grown by MOCVD \odot

B. G. Hagar \square \square ; M. Abdelhamid \square ; E. L. Routh \square ; P. C. Colter; S. M. Bedair



Appl. Phys. Lett. 121, 052104 (2022) https://doi.org/10.1063/5.0103152





CrossMark





Ohmic co-doped GaN/InGaN tunneling diode grown by MOCVD

Cite as: Appl. Phys. Lett. 121, 052104 (2022); doi: 10.1063/5.0103152 Submitted: 14 June 2022 · Accepted: 14 July 2022 · Published Online: 5 August 2022







B. G. Hagar, ^{1,a)} (b) M. Abdelhamid, ¹ (b) E. L. Routh, ² (b) P. C. Colter, ¹ and S. M. Bedair ¹

AFFILIATIONS

 1 Department of Electrical and Computer Engineering, North Carolina State University, Raleigh,North Carolina 27695, USA

ABSTRACT

Tunnel junctions (TJs) have recently been proposed as a solution for several III-nitride current problems and to enhance new structures. Reported III-nitride TJs grown by metalorganic chemical vapor deposition (MOCVD) resulted in backward diodes with rectifying behavior in forward bias, even with Mg and Si doping in 10²⁰ cm⁻³. This behavior limits applications in several device structures. We report a TJ structure based on $p^+In_{0.15}Ga_{0.85}N/n^+In_{0.05}Ga_{0.95}N$, where the n-side of the junction is co-doped with Si and Mg and with electron and hole concentrations in the mid-10¹⁹ cm⁻³ for both the n and p dopants. Co-doping creates deep levels within the bandgap that enhances tunneling under forward biased conditions. The TJ structure was investigated on both GaN substrates and InGaN templates to study the impact of strain on the TJ I-V characteristics. The resulting TJ I-V and resistivities reported indicate the potential for this TJ approach in several device structures based on III-nitrides. We are not aware of any previous MOCVD grown TJs that show Ohmic performance in both forward and reverse biases.

Published under an exclusive license by AIP Publishing. https://doi.org/10.1063/5.0103152

Tunneling diodes/tunnel junctions (TJs) can enable a variety of device structures to improve their performance. TJs were applied in several nitride-compound applications to address issues such as current spreading in the p-GaN layer and hole injection efficiency as well as enabling tandem multiple emitting diodes. 1-3 Additionally, IIInitride based TJs have the potential to enable several device structures by reducing optical losses compared to standard indium tin oxide (ITO) contacts, improving the external quantum effect (EQE) of blue and green light emitting diodes (LEDs), and enabling structures such as multi-junction solar cells.4 Several research groups reported TJs by a variety of different growth techniques, including molecular beam epitaxy (MBE),^{5–8} metalorganic chemical vapor deposition and a hybrid combines both techniques.

The p⁺GaN/n⁺GaN TJs grown by MBE showed superior performance due to the ability of this technique to achieve GaN with the hole concentration in the mid-10¹⁹ cm⁻³.6-8 MOCVD grown GaN research has reported hole concentrations limited to the 10¹⁷ cm⁻³ range. 15 Several groups have also reported InGaN/GaN based TJs, taking advantage of the high piezoelectric field near the junction interfaces.5-7 Such an electric field will result in the reduction of the depletion layer width and, thus, tunneling thickness, which will enhance the tunneling probabilities. Reasonably good TJs were reported with $In_xGa_{1-x}N$ with about $x \sim 0.4$; however, such a high Incontent will complicate integration of these TJs with LEDs due to light absorption in the low bandgap and heavily doped InGaN layers.

Most reported data about TJs deal with the growth of an n-on-p TJ on existing LED structures to reduce the contact resistance by changing the top p-type layer to an n⁺GaN layer.^{3,9–11,14} The presence of the TJ adds a voltage drop to the LED structure ranging from a fraction of a volt to more than one volt depending on the growth approach. $^{3,9-11,14}$ The I–V characteristics of these TJs as isolated structures are only reported in a few studies. 5,6,8,9 Krishnamoorthy et al., Vadiee et al., and Clinton et al. reported MBE grown TJs with conducting properties in both forward and reverse biases by using p⁺In_{0.4}Ga_{0.6}N or by very heavy doping in GaN junctions with mid-10²⁰ cm⁻³ for both the n⁺ and p⁺ doping.^{5,4} 16 Okumura et al. reported GaN based backward diodes grown by MBE with rectifying behavior for forward bias over a large temperature range.⁶ For MOCVD grown TJs, the I-V response behaves as a backward diode with high current achieved at low reverse biased voltages and rectifying I-V in forward bias. Minamikawa et al. reported that in the forward biased direction, a TJ grown by MOCVD showed rectifying nonohmic characteristics in the I-V curve, resulting in a very large voltage drop of 1 V at a current density of 10 A/cm^{2.9} The reverse

²Department of Materials Science and Engineering, North Carolina State University, Raleigh, North Carolina 27695, USA

a) Author to whom correspondence should be addressed: bghagar@ncsu.edu

biased tunnel diode seems to address the problem of highly resistive p-type contacts by following the LED with an n-on-p TJ to take advantage of the superior contacting properties of $n^+ GaN.^{3,9-11,14}$ However, there are several applications in the III-nitride compounds that require connecting junctions in both forward and reverse biases. Examples are multi-junction solar cells and multicolor photo detectors based on the InGaN material system. 4

Inter-band tunneling requires a very thin depletion layer (tunneling width). III-nitrides are expected to have very low inter-band tunneling probabilities due to the difficulty in getting degenerate impurity doping, large effective mass, and relatively high built-in potential barriers.^{6,7} One of the main problems for GaN based TJs is a lack of heavy doping levels using Mg, especially in MOCVD grown structures. Heavy Mg doping with concentration approaching mid-10¹⁹ cm⁻³ and higher is accompanied by the formation of pyramidal defects, inversion domains, and nitrogen vacancies leading to selfcompensation effects. For MOCVD growth, these problems can be alleviated by substituting p-In_xGa_{1-x}N for p-GaN. We have recently reported that the hole concentration increases as a function of the Incontent in p-InGaN, compared to similarly doped p-GaN. 15 However, detrimental optical absorption losses can occur due to the lower bandgap of high In-content InGaN, coupled with band tailing caused by heavy doping effects.

Currently, Mg is the only available p-type dopant for nitride compounds. Mg has several problems that impact the performance of nitride devices, in general, and tunnel junctions, in particular. First, there is delayed Mg incorporation during the initial growth, which is likely due to the time needed to coat the susceptor, reactor tube, etc. 12 Second, Mg shows a memory effect where Mg atoms are incorporated in subsequent layers after the Mg source is switched off.¹⁷ This carryover may be a result of Mg adsorbed on the walls of the reactor. Third, Mg in GaN and other semiconductor compounds have a relatively high diffusion coefficient when exposed to high temperatures. In GaN, Mg atoms have a diffusion coefficient, D, of about 10^{-15} cm²/s¹⁸ leading to a characteristic diffusion length $L = \sqrt{Dt}$, where t is the time exposed to high temperature heating. For the 30 min of heating at 1000 °C needed to grow GaN on the TJ, L can be on the order of 10 nm. 12 This can be irrelevant when dealing with some device structures such as LEDs and lasers. However, for a III-nitride tunnel junction such as GaN, the depletion layer width is close to the tunneling width at about 10 nm;^{1,14} Mg will be present on the n side of the junction either by diffusion or due to memory effects. This will compensate the n type Si dopant and broaden the depletion width by forming a graded junction. The tunneling probability, which depends exponentially on the depletion layer width, is reduced.⁶ Mg diffusion can explain the deterioration of GaN TJs when exposed to high temperature treatments. It has been reported that the voltage drop across the TJ increased by 0.55 V due to thermal treatment. Several of these doping related challenges were addressed in high bandgap conventional (As,P) III-V compounds by the addition of a quantum well at the junction interface and delays in switching on the dopants.²

We report an approach based on several modifications of current processes to reduce or eliminate the previously discussed Mg doping problems related to the growth of TJs based on III-nitride compounds. These modifications can produce a more abrupt doping profile at the TJ interface and result in a TJ more resilient to thermal annealing. First, the n⁺ side of the TJ is co-doped by both Si and Mg. For a

p-on-n TJ, the co-doping of Si and Mg on the n-side of the junction followed by the same Mg concentration in the p-side will eliminate the delay in Mg incorporation that occurs with conventional p+(Mg) on n+(Si) procedures. Widening of the depletion layer due to diffusion or uncontrolled Mg memory effects will not occur, as the same Mg concentration is present on both sides of the TJ. The second modification is to take advantage of the variation in the hole concentration (ionized Mg atoms) with the In-content in InGaN. For example, given a Mg concentration in the mid-10¹⁹ cm⁻³, the hole concentration will be in the mid- 10^{17} cm⁻³ for GaN, and the low 10^{18} cm⁻³ to mid- 10^{19} cm⁻³ for $In_{0.05}Ga_{0.95}N$ and $In_{0.15}Ga_{0.85}N$, respectively. ¹⁵ A heterojunction with an n⁺ layer (Si+Mg) comprised of either GaN or In_{0.05}Ga_{0.95}N, and a p⁺ (Mg) In_{0.15}Ga_{0.85}N layer offers a more abrupt junction interface. Additionally, we do not find it is necessary to use Mg and Si concentrations in the 10²⁰ cm⁻³ range.^{9,14} Doping both sides of the junction to the low to mid-10¹⁹ cm⁻³ range was found to be sufficient for a connecting junction. This should avoid the formation of pyramid like structural defects resulting from such high dopant concentrations. This can be a critical parameter for devices deposited on these TJs in either junction configurations, n-on-p or p-on-n. Kurokawa et al. reported that the non-optimum MOCVD grown TJ impacted the performance of devices grown on these TJs.²³ By addressing these Mg issues, we are able to report a low resistivity under both the forward and reverse biases.

The structures were grown on 5 μ m n-type GaN on sapphire substrates supplied commercially with a dislocation density of $\sim 10^8 \, \text{cm}^{-2}$ using a home-made metal organic chemical vapor deposition (MOCVD) growth system as previously reported.²⁴ In our reactor, the substrate rotates between streams of column-III and column-V gases. The precursors used were trimethylindium (TMIn), trimethylgallium (TMGa), and NH₃. The carrier gases are H₂ and N₂. Bis(cyclopentadienyl)magnesium (Cp2Mg) and silane (SiH4) were used for the p-type and n-type dopants, respectively. Two structures are studied: the first is a TJ grown on GaN and the second on an InGaN semibulk (SB) template. The growth details and the characterizations of these InGaN templates were previously reported.^{24–26} We used the SB approach for growth of these templates where each thick InGaN growth layer is followed by a thin high temperature GaN interlayer to backfill the V-pits generated during the relaxation processes. The In-content in the templates was controlled by varying the growth temperature of the InGaN layer. The TJ is made of n⁺ In_{0.05}Ga_{0.95}N (Si+Mg) with thicknesses in the range of 15–40 nm, followed by a p⁺ In_{0.15}Ga_{0.85}N (Mg) layer 20–40 nm thick. The Mg flow was kept constant during the entire growth of the TJ. Both photoluminescence (PL) and x-ray diffraction (XRD) are used to determine the In-composition based on measurement of thicker grown films. Hall Van der Pauw measurements were used to determine the carrier concentration in both the n⁺ and p⁺ layers. Samples were annealed at 750 °C for 20 min under N_2 ambient for p-type activation. Devices $400 \times 400 \ \mu m^2$ are fabricated using standard techniques: $400 \times 400 \ \mu \text{m}^2$ mesas were etched followed by standard Ohmic n-type and p-type contacts.

The TJ structures shown in Fig. 1 are for the same TJ on different substrates: GaN in Fig. 1(a) and on an InGaN template in Fig. 1(b). The TJ layers on GaN are strained to utilize the added advantages of the piezoelectric field in band bending and narrowing of the depletion layer thickness. PL emission for the TJ shown in Fig. 2(b) at 420 nm is originating primarily from the thicker InGaN template. Based on the

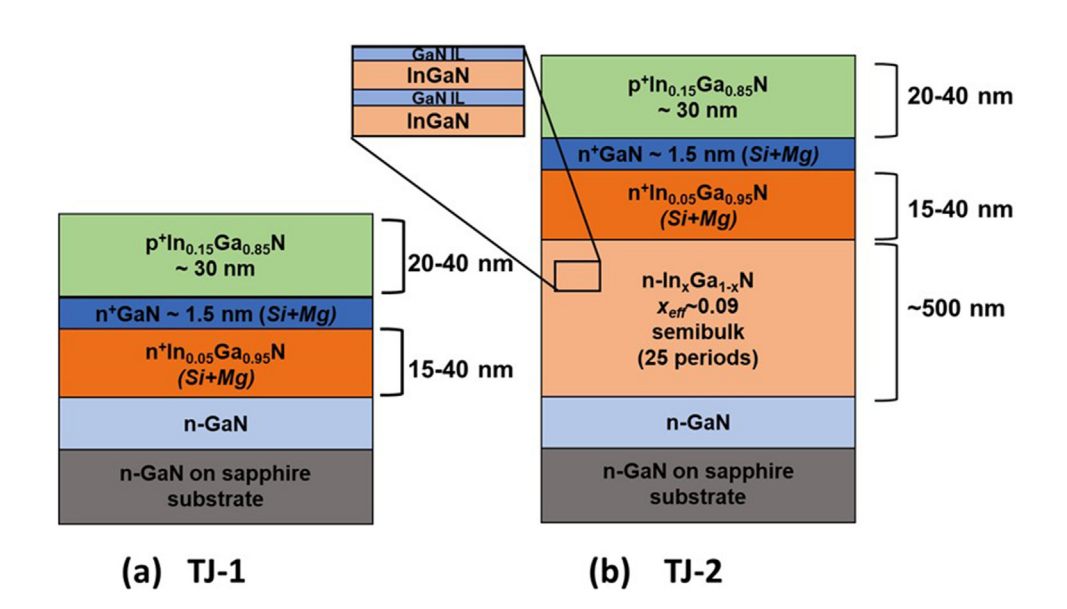


FIG. 1. The schematic representation of (a) TJ-1, a TJ structure on GaN, and (b) TJ-2, the same TJ structure on a 25-period semi bulk, where a period is defined as one cycle of InGaN and a GaN IL.

model presented earlier, the 420 nm emission corresponds to a fully relaxed template with an In concentration of about 9%. The TJs on the InGaN template structure with an In concentration of about 5% and 15% for $\rm n^+$ and $\rm p^+$, respectively, in Fig. 1(b) are expected to be very slightly strained to the relaxed InGaN templates.

Figure 2 represents the I–V characteristics across a small signal [Fig. 2(a)] for TJ-1 (blue) and TJ-2 (red) as well as across a large signal [Fig. 2(b)]. The TJs in both figures have non-rectifying linear Ohmic behaviors in both the forward and reverse bias directions. A wide spread in the I-V of the TJ in both forward and reverse biases is observed. These variations are presented in Fig. 2 by error bars deduced from testing at least ten devices for each plot. This can be due

to a lack of a thick contacting layer as well as slight variations in the thickness and In-composition across the samples, especially for the p^+ $In_{0.15}Ga_{0.85}N$ film, which can be critical in the achieved hole concentrations. Such a lack of uniformity is expected in a home built MOCVD system.

From Fig. 2(a), at a low current, both TJ-1 and TJ-2 show a resistivity of $8\times 10^{-2}~\Omega\cdot cm^2$, indicating no change in resistivity due to the underlying template. On the high current I–V [Fig. 2(b)], for reverse bias, the resistivity is in the range of $5\text{-}6\times 10^{-2}~\Omega\cdot cm^2$. For forward bias of the high current range, the resistivities are 1×10^{-1} and $6\times 10^{-2}~\Omega\cdot cm^2$ for TJ-1 (TJ grown on GaN) and TJ-2 (TJ grown on an InGaN template), respectively. The resistivities deduced from Fig. 2

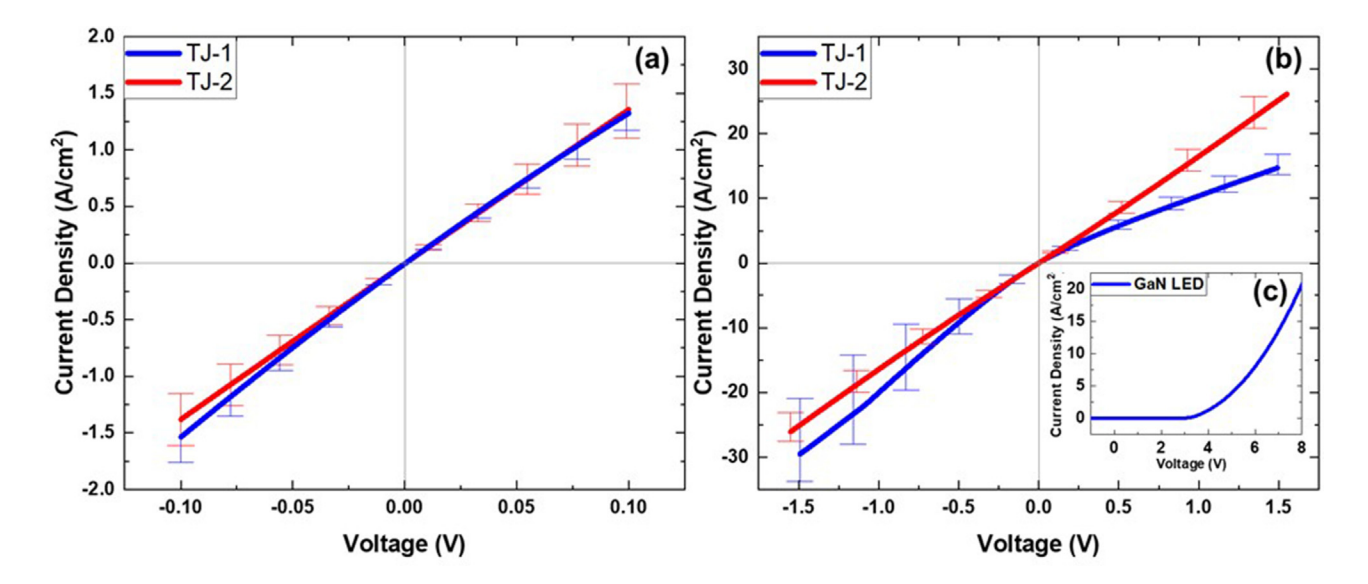


FIG. 2. I–V curves of TJ-1 (blue) and TJ-2 (red) across (a) $-0.1\,\text{V}$ to 0.51 and (b) $-1.5\,\text{V}$ with (c) inset showing IV of the MQW based LED structure using identical mesa and metallization processes.

are the sum of the sheet resistance from both n- and p-type layers, contact resistances, and others. We compared these results with those of our standard InGaN/GaN based MQW LED structures [Fig. 2(c)], which have sources of sheet and contact resistances in common to that of the TJ structures. The resistivity of a previously reported LED structure in the linear part of the I–V curve past 5 V forward bias is about $0.3~\Omega\cdot\text{cm}^2$, which is comparable with the current TJ resistivity shown in Fig. 2. Thus, it is safe to conclude that the current TJ is not expected to add significant extra resistance when incorporated in a device structure. In addition, by comparing the data from Fig. 2, the strained (TJ-1) and barely strained (TJ-2) I–V results indicate that enhancement of the tunneling processes does not seem to be impacted by the PZ field. The tunneling processes are, thus, mainly a function of the deep levels in the bandgap and their concentrations.

For reverse bias, tunneling across the depletion region is taking place due to heavy p+ and n+ doping levels. Electrons tunnel from the filled valence band states in the p+ layer to the empty conduction band states in the n+ layer. For forward bias, the plotted I-V curve in Fig. 2 shows a linear Ohmic behavior, which deviates from previously reported MOCVD grown TJ results (which have a backward diode behavior) by now showing a similar behavior in both forward and reverse directions.

There are several possible reasons for the improved linear connecting properties in the forward direction. First, in this work, the constant Mg concentration across the $\rm n^+$ and $\rm p^+$ layers allowed abrupt electron and hole concentrations at the junction interface. Second, the constant Mg concentration reduces the potential for Mg diffusion to create a wider graded junction. Finally, a third reason is attributed to the Mg doping on the $\rm n+$ side of the TJ. Mg in GaN forms two levels within the bandgap: the Mg acceptor level is about 180–200 meV above the valence band while another deep donor level exists at around 400–440 meV below the conduction band. This deep donor level has been attributed to a Mg and nitrogen vacancy complex (Mg- $\rm V_N$). The transition between those two levels is responsible for the blue band emission, around 2.8 eV, that is typically observed in the heavily doped p-GaN film. $^{15,27-29}$ Similar levels are expected to be present in $\rm n^+In_{0.05}Ga_{0.95}N$ due to the Mg+Si co-doping.

In general, the resistivity of the reverse bias TJ is slightly lower than that in forward bias as shown in Fig. 2(b). It is possible that the charge tunneling (reverse bias) is due to both band-to-band and deep levels within the bandgap. It is very unlikely to have any band-to-band tunneling in forward bias, and only defect assisted tunneling is taking place. This was confirmed by the lack of negative resistance in I–V measurements made at 77 K.

The energy band diagram for the TJ is shown schematically in Fig. 3 with the two Mg levels highlighted. For reverse bias, carriers are tunneling through the reduced-width depletion region. For forward bias, an excess current can be due to energy levels within the bandgap. Heavy doping of both sides of the junction likely initiates these defects. It is very possible that in the forward biased TJ, electrons are tunneling between these N-vacancy levels in the forbidden bandgap of the n-side of the junction to vacant states in the VB of the p-side, as seen in Fig. 3. There may be other sources of deep levels within the bandgap, located on both sides of the junction, which contribute to this high excess current. Several reports suggest that the forward current in most nitride TJs is due to tunneling involving deep levels (i.e., midbandgap levels). ^{16,30} Vadiee *et al.* showed that the valley current, but

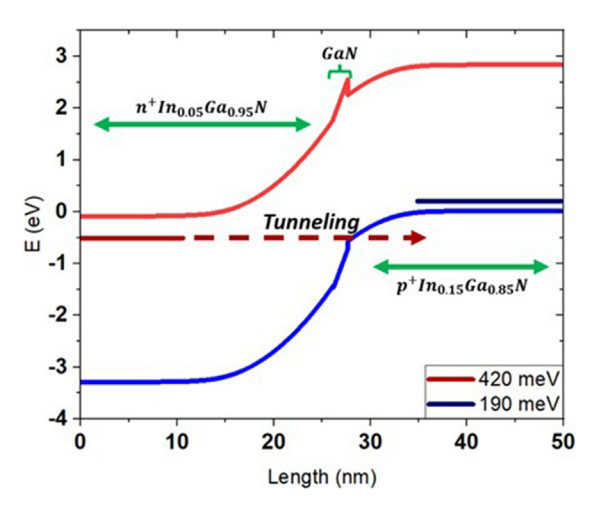


FIG. 3. The energy band diagram schematically represented for the TJ structures.

not the negative resistance related peak current, of their TJs varies approximately as the absolute temperature. We can see a similar temperature dependence in our TJs. ¹⁶ It is fairly well established that valley currents are defect related. At this stage, it can be difficult to pinpoint the exact reasons for these highly desirable properties of this TJ structure. More work needs to be done to investigate these properties of the InGaN films that are simultaneously heavily doped by both Si and Mg.

In general, the resistivity of the reverse bias TJ is slightly lower than that in forward bias as shown in Fig. 2(b). It is possible that the charge tunneling (reverse bias) is due to both band-to-band and deep levels within the bandgap. It is very unlikely to have any band-to-band tunneling in forward bias, and only defect assisted tunneling is taking place. This was confirmed by the lack of negative resistance in I–V measurements made at 77 K.

The integration of TJs into devices can be critical for the development of multi-color LEDs and multi-junction solar cell (MJSC) structures.4 Thus, to highlight the potential of this TJ structure, the photoluminescence (Fig. 4) of an n-on-p device with the incorporation of a buried TJ is compared to that of a traditionally grown MQW on GaN with similar PL emission. The active region of these devices consists of InGaN/GaN multiple quantum wells (MQWs) grown similarly to those described elsewhere. ²⁶ For the MQW on the TJ, the TJ is grown similarly to that of TJ-1, followed by \sim 25 nm of p-GaN. A schematic of this structure can be seen in Fig. 4(b). The active region is then capped with approximately 40 nm of low In-content InGaN, followed by approximately 1-2 nm of n-GaN. For the MQW on GaN, the active region is followed by ~150 nm of p-GaN. The PL was taken using a 405 nm 40 mW laser diode for excitation with the same photomultiplier tube (PMT) voltage for similar spectra comparison. Both MQWs are emitting at approximately 490 nm. For the MQW on the TJ, an additional emission is observed at 444 nm, attributed to the underlying TJ. The emissions were fit with a Gaussian distribution function. The width of the MQW on GaN was found to be (27.0 ± 0.2) nm and (24.8 ± 0.2) nm. As seen by the PL results in Fig. 4(a), we do not see substantial degradation of the PL emission due to the underlying TJ, showing potential for further integration into future devices. These devices are in fabrication and will be reported in the future work.

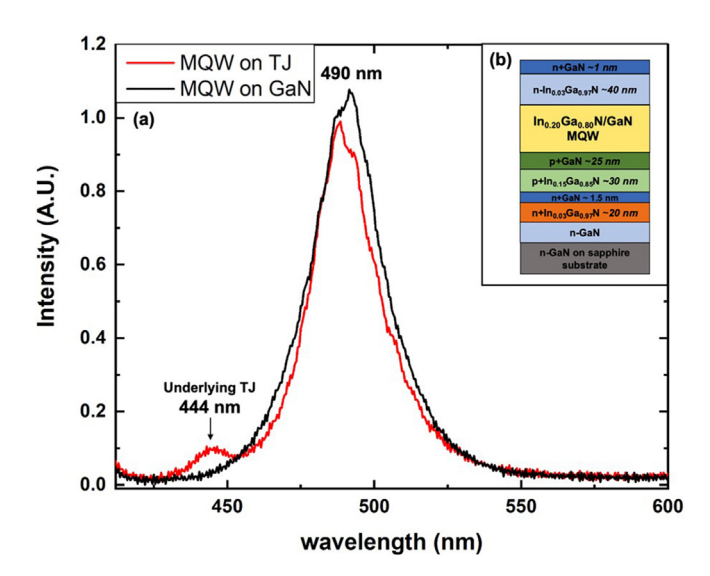


FIG. 4. (a) Photoluminescence of a MQW grown on a TJ structure (red), compared to a similar emitting MQW on GaN (black). (b) Schematic representation of the MQW grown on the TJ structure.

In conclusion, we demonstrate TJs conducting in both forward and reverse biases grown by MOCVD. These results are achieved by addressing several of the Mg problems facing nitride-based TJ structures. We show that co-doping the n-side of the junction with both Si an Mg seems to create deep levels within the bandgap, which enhance tunneling under forward biased conditions. The resulting TJ I–V and resistivities are reported, indicating the potential of this TJ design in several device structures based on III-nitrides. We are not aware of any previous MOCVD grown III-nitride TJs that display linear conduction in both forward and reverse biases.

We would like to acknowledge the Analytical Instrumentation Facility at NCSU for XRD and AFM support. This work was supported by the National Science Foundation under Grant Nos. ECCS-1407772 and ECCS-1833323. This work was performed in part at the Analytical Instrumentation Facility (AIF) of North Carolina State University, which is supported by the State of North Carolina and the National Science Foundation (Award No. ECCS-2025064). The AIF is a member of the North Carolina Research Triangle Nanotechnology Network (RTNN), a site in the National Nanotechnology Coordinated Infrastructure (NNCI). We thank N. E. Routh for his contribution to grammar and syntax.

AUTHOR DECLARATIONS Conflict of Interest

The authors have no conflicts to disclose.

Author Contributions

Brandon G Hagar: Investigation (equal); Methodology (equal); Writing – original draft (equal). **Mostafa Abdelhamid:** Data curation (equal); Formal analysis (equal); Investigation (equal); Methodology (equal); Writing – review and editing (equal). **Evyn Lee Routh:** Data

curation (equal); Formal analysis (equal); Investigation (equal); Methodology (equal); Software (equal); Writing – review and editing (equal). **Peter C. Colter:** Data curation (equal); Formal analysis (equal); Supervision (equal); Validation (equal); Writing – review and editing (equal). **Salah M. Bedair:** Conceptualization (equal); Funding acquisition (lead); Project administration (lead); Writing – original draft (equal).

DATA AVAILABILITY

The data that support the findings of this study are available from the corresponding author upon reasonable request.

REFERENCES

- ¹B. P. Yonkee, E. C. Young, C. Lee, J. T. Leonard, S. P. DenBaars, J. S. Speck, and S. Nakamura, "Demonstration of a III-nitride edge-emitting laser diode utilizing a GaN tunnel junction contact," Opt. Express 24, 7816–7822 (2016).
- ²Z. Jamal-Eddine, B. P. Gunning, A. A. Armstrong, and S. Rajan, "Improved forward voltage and external quantum efficiency scaling in multi-active region III-nitride LEDs," Appl. Phys. Express 14, 092003 (2021).
- ³A. I. Alhassan, E. C. Young, A. Y. Alyamani, A. Albadri, S. Nakamura, S. P. DenBaars, and J. S. Speck, "Reduced-droop green III–nitride light-emitting diodes utilizing GaN tunnel junction," Appl. Phys. Express 11, 042101 (2018).
- ⁴S. Bedair, M. Lamorte, and J. Hauser, "A two-junction cascade solar-cell structure," Appl. Phys. Lett. **34**(1), 38–39 (1979).
- ⁵S. Krishnamoorthy, P. S. Park, and S. Rajan, "Demonstration of forward interband tunneling in GaN by polarization engineering," Appl. Phys. Lett. **99**, 233504 (2011).
- ⁶H. Okumura, D. Martin, M. Malinverni, and N. Grandjean, "Backward diodes using heavily Mg-doped GaN growth by ammonia molecular-beam epitaxy," Appl. Phys. Lett. **108**, 072102 (2016).
- ⁷S. Krishnamoorthy, F. Akyol, P. S. Park, and S. Rajan, "Low resistance GaN/InGaN/GaN tunnel junctions," Appl. Phys. Lett. **102**, 113503 (2013).
- ⁸E. A. Clinton, E. Vadiee, S.-C. Shen, K. Mehta, P. D. Yoder, and W. A. Doolittle, "Negative differential resistance in GaN homojunction tunnel diodes and low voltage loss tunnel contacts," Appl. Phys. Lett. 112, 252103 (2018).
- ⁹D. Minamikawa, M. Ino, S. Kawai, T. Takeuchi, S. Kamiyama, M. Iwaya, and I. Akasaki, "GaInN-based tunnel junctions with high InN mole fractions grown by MOVPE," Phys. Status Solidi B 252, 1127–1131 (2015).
- 10 P. Sohi, M. Mosca, Y. Chen, J.-F. Carlin, and N. Grandjean, "Low-temperature growth of n^{++} -GaN by metalorganic chemical vapor deposition to achieve low-resistivity tunnel junctions on blue light emitting diodes," Semicond. Sci. Technol. **34**, 015002 (2018).
- Z. Jamal-Eddine, S. M. N. Hasan, B. Gunning, H. Chandrasekar, M. Crawford,
 A. Armstrong, S. Arafin, and S. Rajan, "Low voltage drop tunnel junctions grown monolithically by MOCVD," Appl. Phys. Lett. 118, 053503 (2021).
 S. M. N. Hasan, B. P. Gunning, Z. J. Eddine, H. Chandrasekar, M. H. Crawford, A.
- ¹²S. M. N. Hasan, B. P. Gunning, Z. J. Eddine, H. Chandrasekar, M. H. Crawford, A. Armstrong, S. Rajan, and S. Arafin, "All-MOCVD-grown gallium nitride diodes with ultra-low resistance tunnel junctions," J. Phys. D 54, 155103 (2021).
- ¹³ M. Kaga, T. Morita, Y. Kuwano, K. Yamashita, K. Yagi, M. Iwaya, T. Takeuchi, S. Kamiyama, and I. Akasaki, "GaInN-based tunnel junctions in n-p-n light emitting diodes," Jpn. J. Appl. Phys., Part 1 52, 08JH06 (2013).
- ¹⁴S. Neugebauer, M. P. Hoffmann, H. Witte, J. Bläsing, A. Dadgar, A. Strittmatter, T. Niermann, M. Narodovitch, and M. Lehmann, "All metalorganic chemical vapor phase epitaxy of p/n-GaN tunnel junction for blue light emitting diode applications," Appl. Phys. Lett. 110, 102104 (2017).
- ¹⁵E. L. Routh, M. Abdelhamid, P. Colter, N. A. El-Masry, and S. M. Bedair, "Ptype $In_xGa_{1-x}N$ semibulk templates (0.02 < x < 0.16) with room temperature hole concentration of mid- 10^{19} cm⁻³ and device quality surface morphology," Appl. Phys. Lett. **119**, 122101 (2021).
- ¹⁶E. Vadiee, E. A. Clinton, J. V. Carpenter, H. McFavilen, C. Arena, Z. C. Holman, C. B. Honsberg, and W. A. Doolittle, "The role of Mg bulk hyperdoping and delta-doping in low-resistance GaN homojunction tunnel diodes with negative differential resistance," J. Appl. Phys. 126, 083110 (2019).

- ¹⁷J. Ran, X. Wang, G. Hu, J. Wang, J. Li, C. Wang, Y. Zeng, and J. Li, "Study on Mg memory effect in npn type AlGaN/GaN HBT structures grown by MOCVD," Microelectron. J. 37, 583–585 (2006).
- ¹⁸I. S. Romanov, I. A. Prudaev, and V. N. Brudnyi, "Diffusion of magnesium in led structures with InGaN/GaN quantum wells at true growth temperatures 860–980 °C of p-GaN," Russ. Phys. J. 61, 187–190 (2018).
- ¹⁹Y. Kuwano, M. Kaga, T. Morita, K. Yamashita, K. Yagi, M. Iwaya, T. Takeuchi, S. Kamiyama, and I. Akasaki, "Lateral hydrogen diffusion at p-GaN layers in nitride-based light emitting diodes with tunnel junctions," Jpn. J. Appl. Phys., Part 1 52, 08IK12 (2013).
- ²⁰J. P. Samberg, C. Zachary Carlin, G. K. Bradshaw, P. C. Colter, J. L. Harmon, J. B. Allen, J. R. Hauser, and S. M. Bedair, "Effect of GaAs interfacial layer on the performance of high bandgap tunnel junctions for multijunction solar cells," Appl. Phys. Lett. 103, 103503 (2013).
- ²¹S. M. Bedair, J. L. Harmon, C. Z. Carlin, I. E. Hashem Sayed, and P. C. Colter, "High performance as-grown and annealed high band gap tunnel junctions: Te behavior at the interface," Appl. Phys. Lett. 108, 203903 (2016).
- ²²D. Jung, C. A. Parker, J. Ramdani, and S. M. Bedair, "AlGaAs/GaInP heterojunction tunnel diode for cascade solar cell application," J. Appl. Phys. 74, 2090–2093 (1993).
- ²³H. Kurokawa, M. Kaga, T. Goda, M. Iwaya, T. Takeuchi, S. Kamiyama, I. Akasaki, and H. Amano, "Multijunction GaInN-based solar cells using a tunnel junction," Appl. Phys. Express 7, 034104 (2014).

- ²⁴M. Abdelhamid, J. G. Reynolds, N. A. El-Masry, and S. M. Bedair, "Growth and characterization of $\text{In}_x\text{Ga}_{1-x}\text{N}$ (0 < x < 0.16) templates for controlled emissions from MQW," J. Cryst. Growth 520, 18–26 (2019).
- 25E. L. Routh, M. Abdelhamid, N. A. El-Masry, and S. M. Bedair, "Device quality templates of In_xGa_{1-x}N (x<0.1) with defect densities comparable to GaN," Appl. Phys. Lett. 117, 052103 (2020).</p>
- ²⁶M. Abdelhamid, E. L. Routh, B. Hagar, and S. M. Bedair, "Improved LED output power and external quantum efficiency using InGaN templates," Appl. Phys. Lett. 120, 081104 (2022).
- 27O. Gelhausen, M. R. Phillips, E. M. Goldys, T. Paskova, B. Monemar, M. Strassburg, and A. Hoffmann, "Dissociation of H-related defect complexes in Mg-doped GaN," Phys. Rev. B 69(12), 125210 (2004).
- ²⁸U. Kaufmann, M. Kunzer, M. Maier, H. Obloh, A. Ramakrishnan, B. Santic, and P. Schlotter, "Nature of the 2.8 eV photoluminescence band in Mg doped GaN," Appl. Phys. Lett. **72**, 1326–1328 (1998).
- 29 U. Kaufmann, M. Kunzer, H. Obloh, M. Maier, C. Manz, A. Ramakrishnan, and B. Santic, "Origin of defect-related photoluminescence bands in doped and nominally undoped GaN," Phys. Rev. B 59(8), 5561–5567 (1999).
- 30 Y. Robin, Q. Bournet, G. Avit, M. Pristovsek, Y. André, A. Trassoudaine, and H. Amano, "Limitation of simple np-n tunnel junction based LEDs grown by metal-organic vapor phase epitaxy," Semicond. Sci. Technol. 35, 115005 (2020).